

Spectral characteristics of ground components one year after fire in an interior Alaskan black spruce forest

Keiji KUSHIDA
Institute of Low Temperature Science
Hokkaido University, Japan

Abstract

Our final goals are to understand component spectral characteristics of black spruce fire chronosequence in interior Alaska, and to model and evaluate detectability of vegetation changes after fire and according carbon budget changes from remotely sensed data. In 2005, the spectral reflectances in 350 – 2500 nm were measured at 80 points (155 samples) in an interior Alaskan black spruce forest (Poker Flat site), which was burned in the summer of 2004, and analyzed the spectral separativeness of the representative ground components (burnt sphagnum mosses, damaged sphagnum mosses, live sphagnum mosses). The points were situated in or around the sixteen 10 m × 10 m plots established by Tsuyuzaki et al. For observing damaged sphagnum mosses and live sphagnum mosses, surface undergrowths on the mosses of the measurement points were removed. The spectral reflectances at all of the points were measured under entirely diffuse illumination conditions. When the solar illumination was specular, an artificial shadow was made on the objects and the reference panel. The spectral reflectances of 21 cases were observed under both specular and diffuse illuminations. As a result, we obtained spectral characteristics of burnt sphagnum mosses, damaged sphagnum mosses, and live sphagnum mosses, and the three had a significant difference. Further, the arial ratio of the ground componsnets were estimated by using the spectral characteristics and Landsat ETM+ imagery (resolution: 15 m – 30 m) taken on 4 Aug. 2004. The results can be used for base information to interpret MODIS (250 m – 1 km), and ALOS (2.5 m – 10 m) satellite data.

1. INTRODUCTION

Recent increase of forest fire in boreal forests in North America and Siberia causes environmental changes in the ecosystems, affecting global climate warming through greenhouse gases emission during the combustion and carbon dioxide and methane release after the fire (Hinzman et al., 2003). Remotely sensed data is useful for fire detection in a wide area, and hence, contribute to the estimation of the fire influence. For this purpose, not only burnt area estimation, but also monitoring of ecosystem and greenhouse gases budget changes after the fire is necessary.

Detection algorithms for boreal forest fires using NOAA AVHRR have been studied and the detachabilities have been evaluated (Flannigan et al., 1986; Cahoon et al., 1992;

Kasischke et al., 1993; Cahoon et al., 1994; Chuvieco et al., 1994; French et al., 1995; Fang and Huang, 1998; Galindo et al., 2003; Soja et al., 2004; Sukhinin et al., 2004; Kucera et al., 2005). These algorithms were based on thermal and mid-infrared bands, and in some cases, the thermal and mid-infrared bands were combined with visible to near-infrared bands to evaluate turning black from vegetation colors.

On the other hands, burn severity or vegetation recovery mapping of boreal forest fires with satellite remote sensing data have been studied since more recent time and in less number of studies in spite of the importance from the viewpoint of the greenhouse gas budgets. One of the reasons for this is that NOAA AVHRR, which covers continental scale twice a day, does not have $2\ \mu\text{m}$ and adjacent wavelength bands, which is effective for the characteristics of burnt scars. Nevertheless, Landsat TM and ETM+, which cover every area in the globe once fourteen days with 30m resolutions, has the $2.09 \sim 2.35\ \mu\text{m}$ band (Band 7). White et al. (1996) and van Wagendonk et al. (2004) used the Landsat band as to evaluate the burn in the USA mainland. There are very few studies on burn severity or vegetation recovery mapping in boreal forests except in interior Alaska (Eptinga et al., 2005). They used Landsat TM and ETM+ for fire severity mapping, and proposed an appropriate remote sensing index for estimating a ground-observed composite burn index (CBI). The CBI was originally proposed as a general index for burn severity evaluation in Montana, and not specialized for the effect on the greenhouse gases emission from boreal forests, though Eptinga et al. (2005) modified the index for use in Alaskan boreal forest. In this study, we based on the field spectral observation of ground components as to evaluate burn severity of interior Alaskan black spruce forest. The ground components have different net primary productivities (NPP), and hence, area ratios of the ground components contribute to the carbon budget of the ground. Moreover, the area ratios influences not only carbon budget just after fire, but also recoveries of the vegetation.

The objectives are to understand component spectral characteristics of black spruce forest in interior Alaska, and to evaluate the burn severity with indicated relationship with carbon budget from remotely sensed data.

2. METHODS

The spectral reflectances in 350 – 2500 nm were measured in a black spruce (*Picea mariana*) forest (Poker Flat site) burnt in the end of June 2004. Almost the entire forest floor was once covered with a moss (*Sphagnum spp.*) seat, and burnt into patches of mosses, damaged mosses, and burnt scars in 10 cm – 10 m scales. We measured spectral reflectance at 80 points (155 samples) in 7 – 13 August 2005 in the site (Table 1). The points were situated in or around the sixteen 10 m \times 10 m plots established by Tsuyuzaki et al. (in this proceedings). We set the three ground components as moss damaged moss, and burnt. A GER

2600 spectral radiometer (GER Corp., New York) was used, and reflectances of 0.15-m-diameter circles to the nadir direction at wavelengths in the 1.5-nm interval in 350 – 1050-nm and the 11.5-nm interval in 1050 – 2500 nm were observed by measuring emissions from the objects and a standard reflectance panel named Spectralon (Labsphere, Inc., North Sutton, United States) alternately at least 5 times. The time period of one emission measurement is about 3 – 5 s. When the solar illumination was fluctuating, the reflectance measurements at one point were repeated up to 10 times, five measurements that have similar reflectance values were chosen, and the others were eliminated. The coefficient of variations of the reflectance factors measured at each of the points were less than 3% in 350 – 1050 nm and less than 15% in 1050 – 2500 nm after diminishing noises by integrating each five neighbor wave bands. Each reflectance measurement consisted of 118 sampled wave bands. For observing “Moss” and “ Damaged moss” (**Table 1**), surface undergrowths on the mosses of the measurement points were removed. All of the spectral reflectance was measured under entirely diffuse illumination conditions. When the solar illumination is specular, an artificial shadow was made on the objects and the reference panel. The spectral reflectances of some points were observed under both specular and diffuse illuminations (**Table 1**). The reflectance panel is corrected with a BaSO₄ standard.

3 RESULTS AND DISCUSSIONS

As a result of the component spectral measurements, the three components, which are moss, damaged moss, and burnt, were different spectral characteristics as shown in **Fig.1**. The averages include all the samples of direct and scattered solar illumination, and vegetation on the mosses removed and not removed. The burnt area has low reflectance throughout the observed wavelength, though in wavelength corresponding to Landsat ETM+ band 7, the burnt area had higher reflectance than the moss and lower reflectance than the damaged mosses. **Table 2** shows the component reflectances in Landsat ETM+ bands. Among the six Landsat ETM+ bands (band 6 is thermal band), the bands 7 and 4 are the two of the most appropriate to distinguish the three components. The index calculated by dividing the band 7 by the band 4 gave separation between the moss and the group composed by the damaged mosses and the burnt. The use of the band ratio can reduce the atmospheric effect in satellite observations more than single bands and used as a burnt severity index in the previous studies (White et al., 1996; van Wagendonk et al., 2004; Eptinga et al., 2005), though the separation between the damaged mosses and the burnt was difficult using the index. By assuming the three components distributes horizontally and eliminating the effect of burned trees, from the result of the spectral measurements, we obtained the follows:

$$C_m = 0.027B_4 - 0.021B_7 + 0.17, \quad (1)$$

$$C_{dm} = 0.04B_4 + 0.14B_7 - 3.9, \quad (2)$$

$$C_b = -0.067B_4 - 0.12B_7 + 4.7, \quad (3)$$

where, C_m , C_{dm} , C_b are area ratios of the mosses, the damaged mosses, and the burnt, and B_4 and B_7 are atmospherically corrected reflectance in Landsat ETM+ bands 4 and 7. These parameters were used for mapping the burned severity on Landsat ETM+ imagery taken on 4 Aug. 2004 (path: 68, row: 15).

Table 1. Number of samples for spectral observation

() denotes the number of samples for observations under both specular and diffuse illuminations.

Plot	Burnt scar	Vegetation on burnt scar	Damaged moss	Vegetation on damaged moss	Moss	Vegetation on moss
L1					5	5
L2					5	5
L3					5(4)	5(4)
L4					4	4
M1	1(1)		4(2)	4(1)		
M2	1(1)		2(2)	2(2)	2(2)	2(2)
M3	2			3		
M4	2			3		
H1	5(5)					
H2	1	3	1	1		
H3		5				
H4	3	1		1		
S1		5				
S2	1	4				
K1		4(4)	1(1)	1(1)		
K2			5(5)	5(5)		
Total	16(7)	22(4)	13(10)	20(9)	21(6)	21(6)

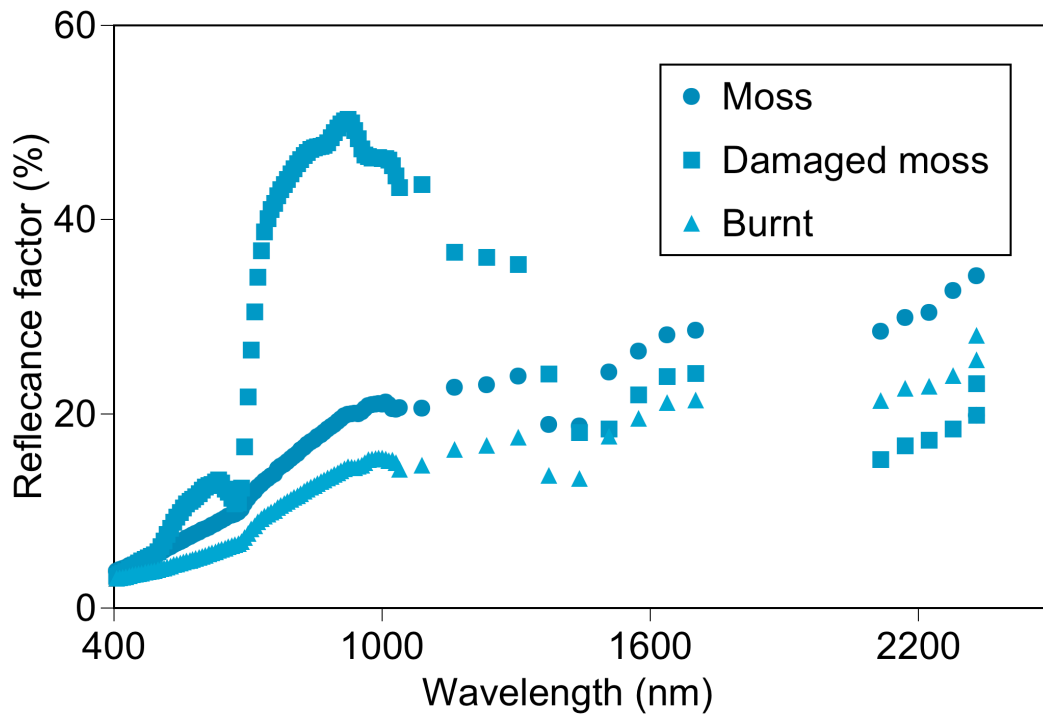


Fig.1. Spectral characteristics ground components of interior Alaskan black spruce forest one year after fire

Table 2. Field-observed spectral characteristics one year after fire of black spruce forest in Landsat ETM+ bands (Average \pm S.D., Unit: %, Numbers of samples are; Moss: 42, Damaged moss 33, Burnt: 38)

Band	Wavelength	Moss	Damaegd moss	Burnt
Band1	0.45 \sim 0.52 μ m	5.2 \pm 2.1	5.8 \pm 1.8	4.0 \pm 1.5
Band2	0.53 \sim 0.61 μ m	9.8 \pm 4.4	8.1 \pm 3.6	5.5 \pm 2.2
Band3	0.63 \sim 0.69 μ m	14.7 \pm 10.0	18.8 \pm 7.1	9.0 \pm 4.0
Band4	0.75 \sim 0.90 μ m	42.3 \pm 14.6	16.8 \pm 8.2	12.3 \pm 6.7
Band5	1.55 \sim 1.75 μ m	23.0 \pm 9.9	28.8 \pm 11.1	21.2 \pm 10.8
Band7	2.09 \sim 2.35 μ m	19.2 \pm 9.6	31.7 \pm 10.0	25.5 \pm 7.1
$\frac{\text{Band7}}{\text{Band4}}$	-	0.45 \pm 0.05	2.1 \pm 0.6	2.4 \pm 0.8

4 CONCLUSIONS

We measured spectral reflectance from three main components one year after interior Alaskan black spruce fire, and proposed Landsat ETM+ band 7 divided by Landsat ETM+ band 4 as an index that indicate the area ratio of the ground components and evaluate burnt severity from the viewpoint of the carbon budget and the forest recovery. The index was used for evaluating the fire severity of 2004 interior Alaskan forest fire with a Landsat ETM+ image.

In the previous study, we built a remote-sensing method for determining leaf area index (LAI) and ground cover mosses/lichens in interior Alaskan spruce forests by field component spectral observation and radiative transfer modeling based on the spectrum (Kushida et al., 2004). The method was applied to evaluate annual net ecosystem productivity (NEP) distribution in a black spruce forest, interior Alaska, by accounting for net primary productivity (NPP) of the vegetation compositions and soil respiration observation synchronized to the spectral observation. Along this methodology, inclusion of ground component spectrum just after fire and knowledge on carbon budget based on the component contributes to evaluate the fire severity in the context of carbon budget. The results can be used for base information to interpret MODIS (250 m – 1 km), and ALOS (2.5 m – 10 m) satellite data.

REFERENCES

- Cahoon, D.R., B.J. Stocks, J.S. Levine, W.R. Cofer, and C.C. Chung (1992), Evaluation of a Technique for Satellite-Derived Area Estimation of Forest-Fires, *J. Geophys. Res.-Atmos.*, 97(D4), 3805-3814.
- Cahoon, D.R., B.J. Stocks, J.S. Levine, W.R. Cofer, and J.M. Pierson (1994), Satellite Analysis of the Severe 1987 Forest-Fires in Northern China and Southeastern Siberia, *J. Geophys. Res.-Atmos.*, 99(D9), 18627-18638.
- Chuvieco, E., and M.P. Martin (1994), A Simple Method for Fire Growth Mapping Using AVHRR Channel-3 Data, *International Journal of Remote Sensing*, 15(16), 3141-3146.
- Epting, J., D. Verbyla, and B. Sorbel (2005), Evaluation of remotely sensed indices for assessing burn severity in interior Alaska using Landsat TM and ETM+, *Remote Sensing of Environment*, 96(3-4), 328-339.
- Fang, M., and W. Huang (1998), Tracking the Indonesian forest fire using NOAA/AVHRR images, *International Journal of Remote Sensing*, 19(3), 387-390.
- Flannigan, M.D., and T.H. Vonderhaar (1986), Forest-Fire Monitoring Using NOAA Satellite AVHRR, *Can. J. For. Res.-Rev. Can. Rech. For.*, 16(5), 975-982.
- French, N.H.F., E.S. Kasischke, L.L. Bourgeauchavez, and D. Berry (1995), Mapping the Location of Wildfires in Alaskan Boreal Forests Using AVHRR Imagery, *Int. J. Wildland*

- Fire, 5(2), 55-62.
- Galindo, I., P. Lopez-Perez, and M. Evangelista-Salazar (2003), Real-time AVHRR forest fire detection in Mexico (1998-2000), *International Journal of Remote Sensing*, 24(1), 9-22.
- Hinzman, L.D., M. Fukuda, D.V. Sandberg, F.S. Chapin, and D. Dash (2003), FROSTFIRE: An experimental approach to predicting the climate feedbacks from the changing boreal fire regime, *J. Geophys. Res.-Atmos.*, 108(D1)
- Kasischke, E.S., N.H.F. French, P. Harrell, N.L. Christensen, S.L. Ustin, and D. Barry (1993), Monitoring of Wildfires in Boreal Forests Using Large-Area AVHRR NDVI Composite Image Data, *Remote Sens. Environ.*, 45(1), 61-71.
- Kucera, J., Y. Yasuoka, and D.G. Dye (2005), Creating a forest fire database for the Far East of Asia using NOAA/AVHRR observation, *International Journal of Remote Sensing*, 26(11), 2423-2439.
- Kushida, K., Y. Kim, N. Tanaka, and M. Fukuda (2004), Remote sensing of net ecosystem productivity based on component spectrum and soil respiration observation in a boreal forest, interior Alaska, *J. Geophys. Res.*, 109, D06108, doi:10.1029/2003JD003858.
- Levine, J.S., W.R. Cofer, D.R. Cahoon, and E.L. Winstead (1995), Biomass Burning - a Driver for Global Change, *Environ. Sci. Technol.*, 29(3), A120-A125.
- Liew, S.C., A. Lim, and L.K. Kwoh (2005), A stochastic model for active fire detection using the thermal bands of MODIS data, *Geoscience and Remote Sensing Letters, IEEE*, 2(3), 337-341.
- Soja, A.J., A.I. Sukhinin, D.R. Cahoon, H.H. Shugart, and P.W. Stackhouse (2004), AVHRR-derived fire frequency, distribution and area burned in Siberia, *International Journal of Remote Sensing*, 25(10), 1939-1960.
- Sukhinin, A.I., N.H.F. French, E.S. Kasischke, J.H. Hewson, A.J. Soja, I.A. Csiszar, E.J. Hyer, T. Loboda, S.G. Conrad, V.I. Romasko, E.A. Pavlichenko, S.I. Miskiv, and O.A. Slinkina (2004), AVHRR-based mapping of fires in Russia: New products for fire management and carbon cycle studies, *Remote Sens. Environ.*, 93(4), 546-564.
- van Wageningen, J.W., R.R. Root, and C.H. Key (2004), Comparison of AVIRIS and Landsat ETM+ detection capabilities for burn severity, *Remote Sensing of Environment*, 92(3), 397-408.
- White, J.D., K.C. Ryan, C.C. Key, and S.W. Running (1996), Remote sensing of forest fire severity and vegetation recovery, *International Journal of Wildland Fire*, 6(3), 125-136.